Circular STAP Research Results

Donald Tufts, Timothy Toolan, Richard Vaccaro

University of Rhode Island
Department of Electrical Engineering
4 East Alumni Avenue
Kingston, RI 02881

tufts@ele.uri.edu, toolan@ele.uri.edu, vaccaro@ele.uri.edu

REPORT DOCUMENTATION PAGE

Form Approved
OMB No. 0704-0188

1. REPORT DATE *(DD-MM-YYYY)* 15-06-2001	**2. REPORT ~~DATE~~** Type Final	**3. DATES COVERED** *(From - To)* May -December 1999

4. TITLE AND SUBTITLE
Space-Time Signal Processing for Circular Ring Arrays

5a. CONTRACT NUMBER

5b. GRANT NUMBER
N00014-99-1-0688

5c. PROGRAM ELEMENT NUMBER

6. AUTHOR(S)
Donald W. Tufts
Timothy Toolan
Richard J. Vaccaro

5d. PROJECT NUMBER

5e. TASK NUMBER

5f. WORK UNIT NUMBER

7. PERFORMING ORGANIZATION NAME(S) AND ADDRESS(ES)
Department of Electrical & Computer Engineering
University of Rhode Island
Kingston, RI 02881

8. PERFORMING ORGANIZATION REPORT NUMBER

9. SPONSORING/MONITORING AGENCY NAME(S) AND ADDRESS(ES)
Office of Naval Research Regional Office Boston
495 Summer St., Room 627
Boston, MA 02210-2109

10. SPONSOR/MONITOR'S ACRONYM(S)
ONR

11. SPONSORING/MONITORING AGENCY REPORT NUMBER

12. DISTRIBUTION AVAILABILITY STATEMENT

Approved for public release

13. SUPPLEMENTARY NOTES

14. ABSTRACT
Describes improvements in fast subspace initialization and tracking and introduces the Back Scattering Inverse (BSI)method for approximate transformation of line-array data into corresponding circular-array segment data, or vice-versa.

15. SUBJECT TERMS
Circular Array; space-time signal processing; STAP; subspace tracking.

16. SECURITY CLASSIFICATION OF: a. REPORT	b. ABSTRACT	c. THIS PAGE	**17. LIMITATION OF ABSTRACT**	**18. NUMBER OF PAGES**	**19a. NAME OF RESPONSIBLE PERSON** Donald W. Tufts
U	U	U	UU	16	**19b. TELEPONE NUMBER** *(Include area code)* (402) 874-5812

Improvements in Fast Subspace Initialization and Tracking

- Original FAST
  - FAST Algorithm (Tufts, Real, Cooley, ICASSP 97, IEEE Trans 99)
  - Tracks dimension, principal singular values, and principal singular vectors of signal or interference subspace from single column matrix updates
  - Uses rectangular windowed data support for fast discarding of edges or ending components
- Recently Improved FAST
  - Removed latency in initialization by a FAST start for FAST
  - Increased speed through multiple column update

A FAST Start for FAST

- Uses same algorithm for initialization and regular operation
- Starts processing data before the full matrix is formed
- When FAST receives final column for initialization, only one FAST iteration is required

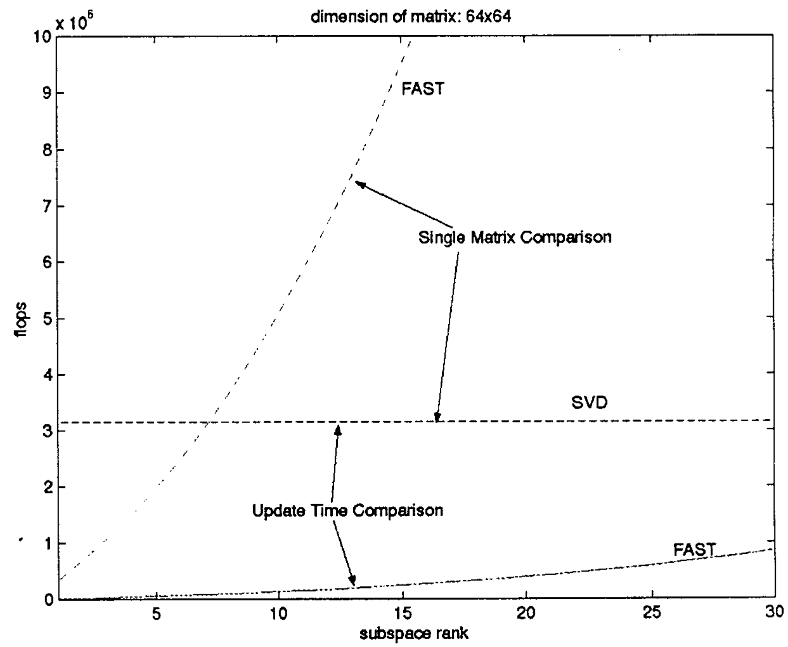

Flops vs. Subspace Rank for a 64x64 matrix

OLD

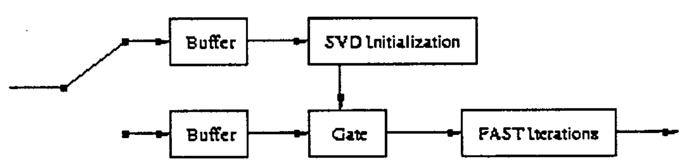

NEW

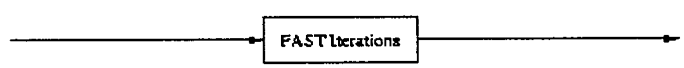

FAST Start for FAST: Event Time Interpretation

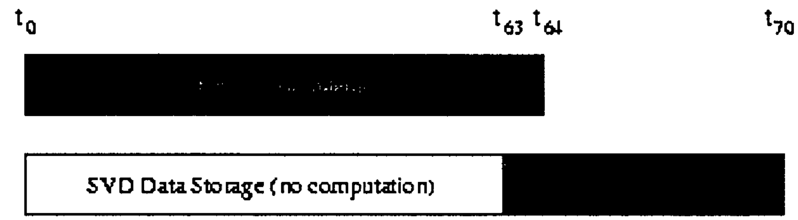

- t_0 : first column of 64x64 matrix arrives
- t_{63} : last column of 64x64 matrix arrives
- t_{64} : FAST iterations for initialization complete and update for new 65th column begins
- t_{70} : SVD initialization for FAST is complete and data between t_{64} and t_{70} has been buffered (exact time, in units of a FAST iteration, depend on signal subspace rank)

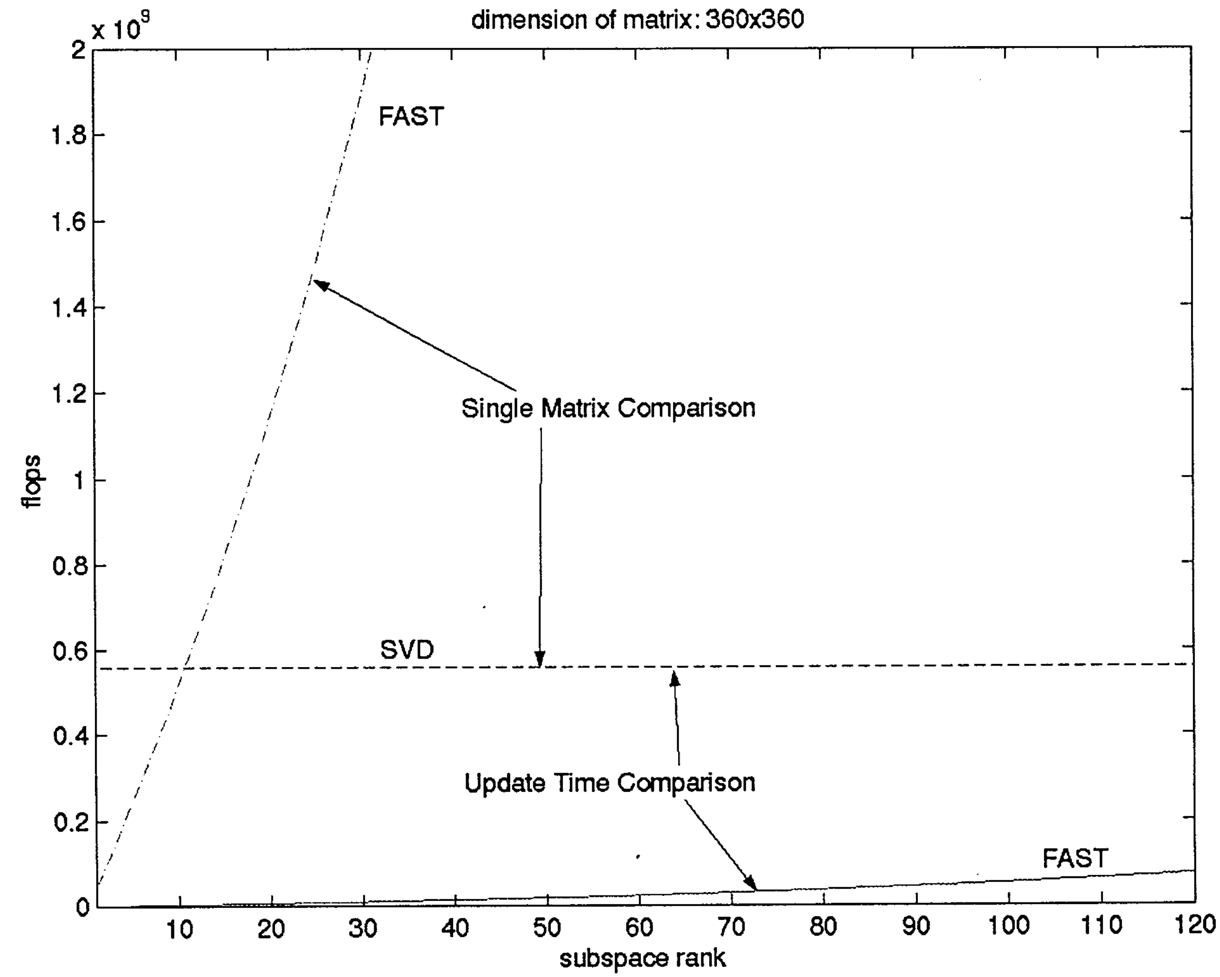

Flops vs. Subspace Rank for
a) Forming the reduced rank singular vectors and singular values for a single isolated 360x360 matrix
b) Updating the singular vectors and singular values for a new overlapping 360x360 matrix

Multicolumn Processing to Reduce Operation Count

- If the data is quasi-stationary over longer periods, then the FAST computations can be reduced using multi-column strides
- Alternatively, tracking a large dimension subspace could exceed the computational capability of a given system. The multicolumn-stride version of FAST can reduce computations, perhaps sacrificing some tracking fidelity.

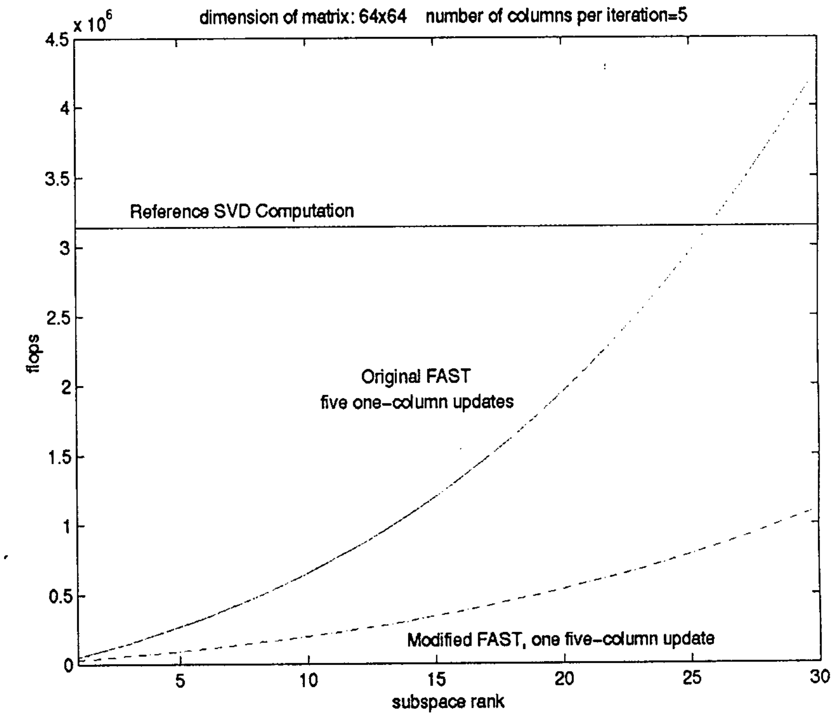

Subspace rank vs. flops for a 64x64 matrix with 5 new columns per iteration.

The Back Scattering Inverse (BSI) Method

- For approximate transformation of line-array data into corresponding circular-array segment data or vice-versa.
  - Basic Principle: Arrange the beamforming of the virtual target array to view the same clutter patches in range with the same resolution as the beams of the source array; then convert source-array beam data to virtual target-array element data.
- For clutter suppression with minimal signal loss, by concentration of clutter in a subspace of low dimension.
  - Given platform velocity, array segment orientation, and crab angle, isodop loci on the ground can be formed.
  - Form sequences of measurements from clutter patches which move out in range along an isodop.
  - Demodulate the isodop beams, each with it's own doppler.
  - Invert demodulated beams to obtain low-resolution clutter-patch matrix.
  - Obtain low rank approximation.

Concentration of Clutter in a Subspace of Low Dimension: Example of Line Array

- MNx1 space-time data vector (M PRI's, N elements, one fixed range R) can be represented by low-resolution, N-coefficient clutter
- Based on Ward's V_c matrix (p. 188) we form the following high-resolution data vector representation

$$V_c = \begin{bmatrix} V_0(N_c) \\ V_1(N_c) \\ \vdots \\ V_{M-1}(N_c) \end{bmatrix} \qquad d = \begin{bmatrix} d_0 \\ d_1 \\ \vdots \\ d_{M-1} \end{bmatrix} = \begin{bmatrix} V_0(N_c) \\ V_1(N_c) \\ \vdots \\ V_{M-1}(N_c) \end{bmatrix} c_m(N_c)$$

MNxN_c space-time steering vectors

MNx1 element data

MNxN_c
N_c>>N

N_cx1 high-res clutter

$m = 0,1,\cdots M-1$

Future Work

- Develop Adaptive Monopulse processing for estimation of arrival angles using segments of a circular array.
- Continue Theoretical and Simulation Work on dimension reducing transformations.
- Continue Work on Chameleon Arrays, that is approximating data from circular array segment using real line array data.
- Work with real data sets from NRL, MCARM, and Mountaintop until real circular array data is available.
- Include real or simulated terrain scattered jamming as well as clutter.

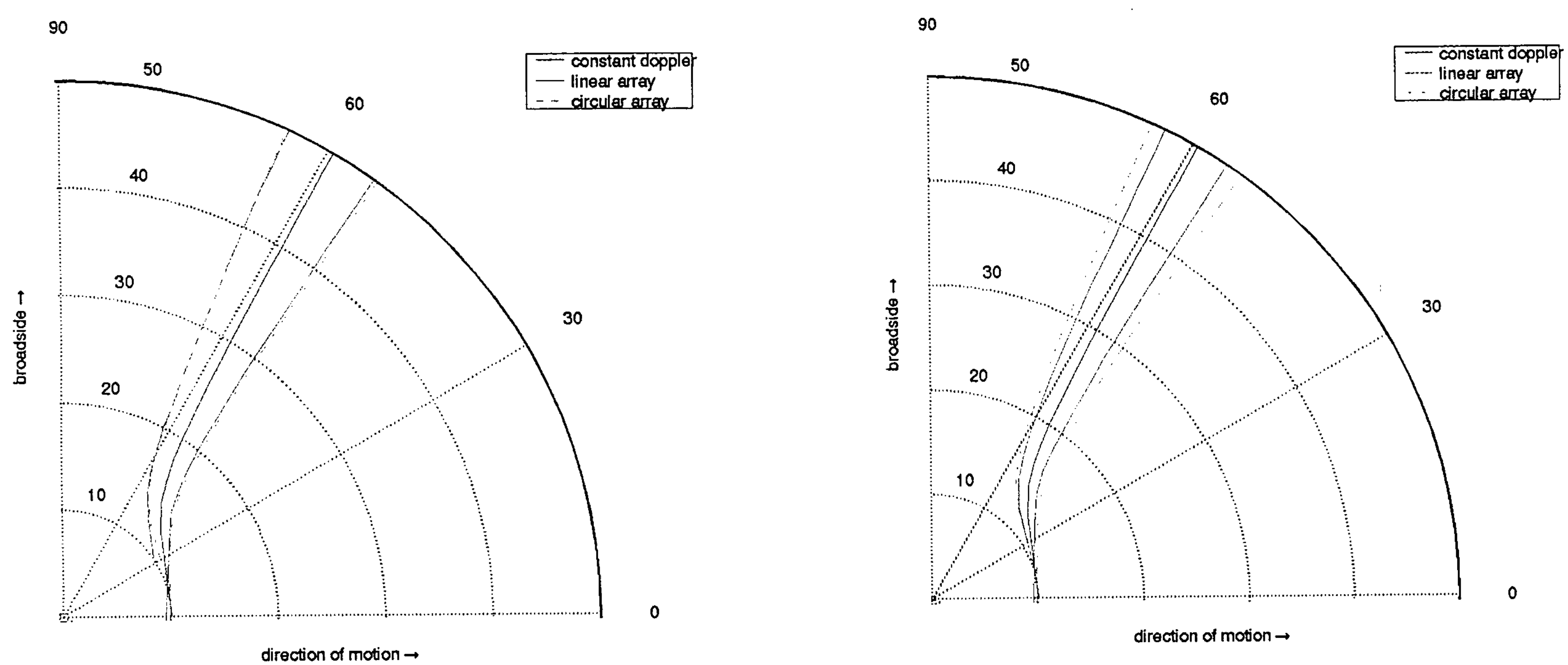

Receive Beam, isodop following sensitivity regions on the ground for side-looking line-array and corresponding circular array segment (using parameters of CSTAP data). The left figure is for a 20 element circular arc and a 15 element line array. The right figure is for a 20 element circular arc and a 20 element line array.

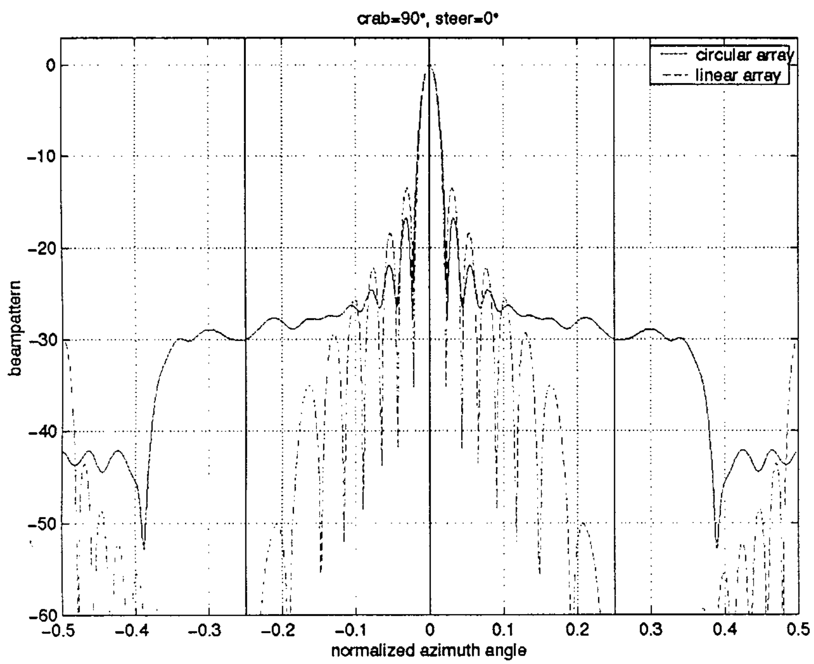

20 element circular array segment
15 element line array segment

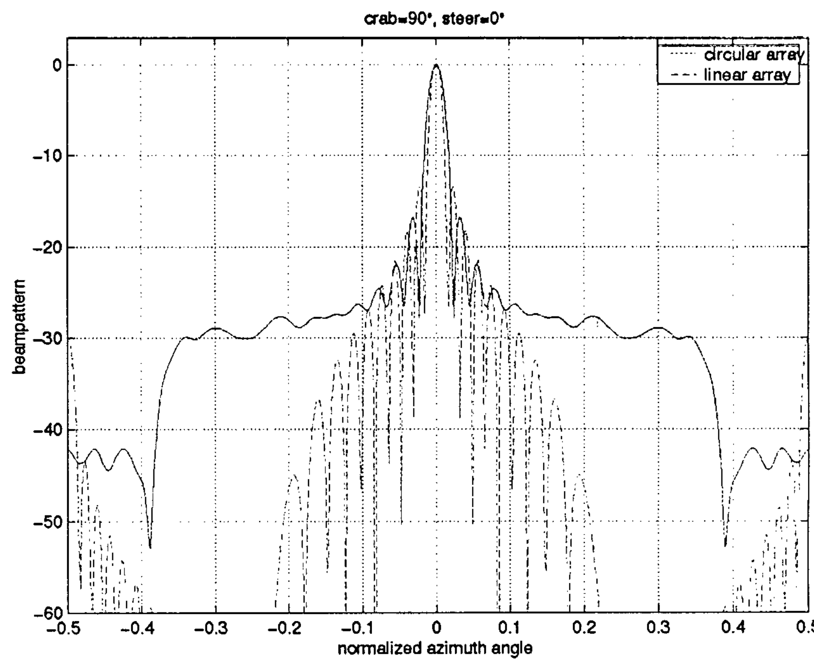

20 element circular array segment
20 element line array segment

Both the main lobe and the side lobes of the 15 element line array segment and the 20 element circular array segment match well. The 20 element line array segment mainlobe is much narrower than the 20 element circular array segment.

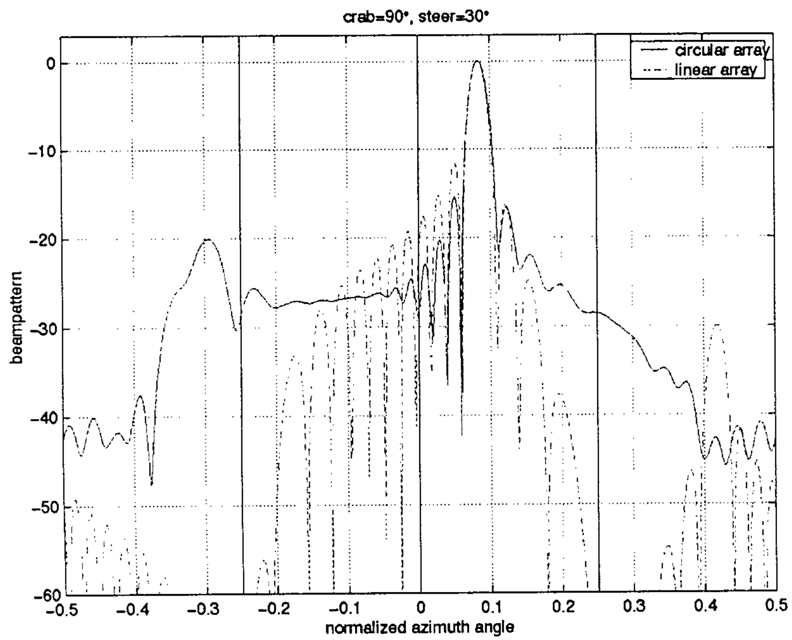

20 element circular array segment
15 element line array segment

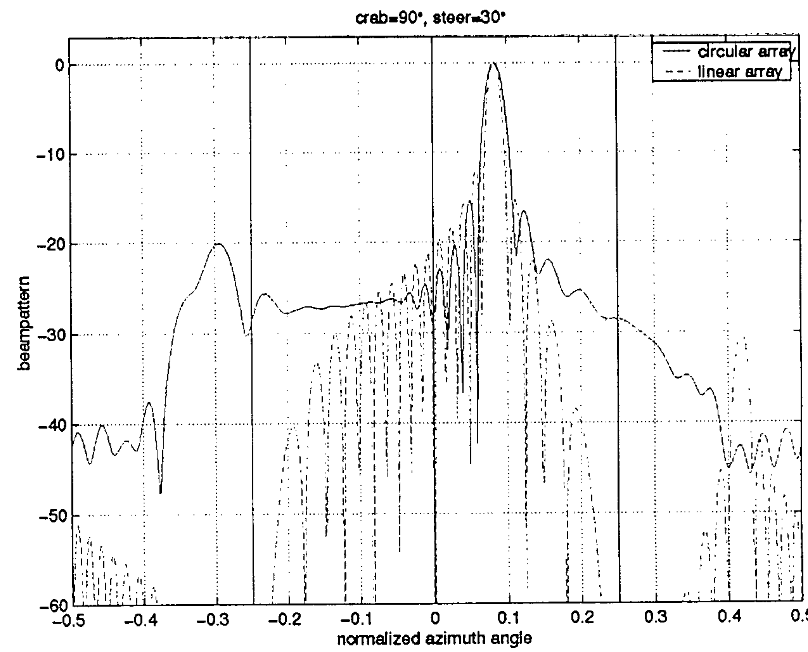

20 element circular array segment
20 element line array segment

Both the main lobe and the side lobes of the 15 element line array segment and the 20 element circular array segment match well. The 20 element line array segment mainlobe is much narrower than the 20 element circular array segment.

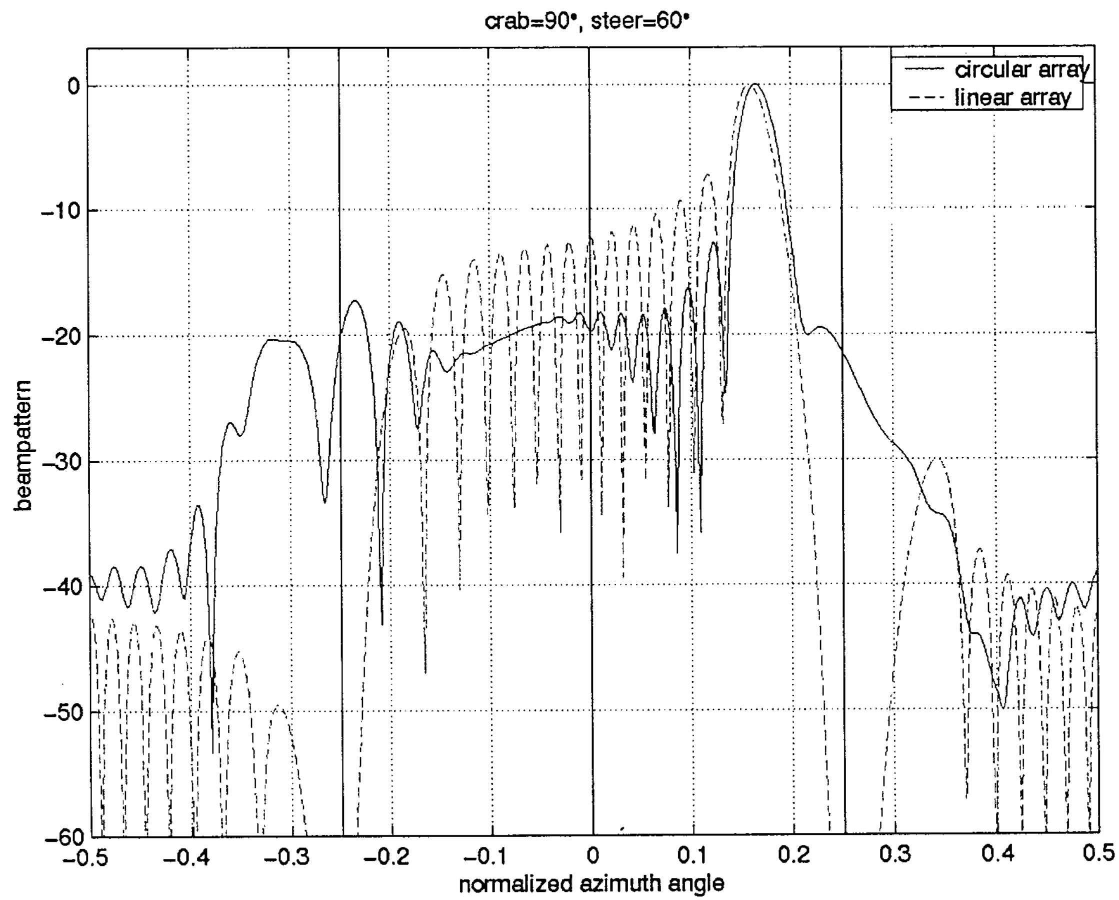

20 element circular array segment
15 element line array segment

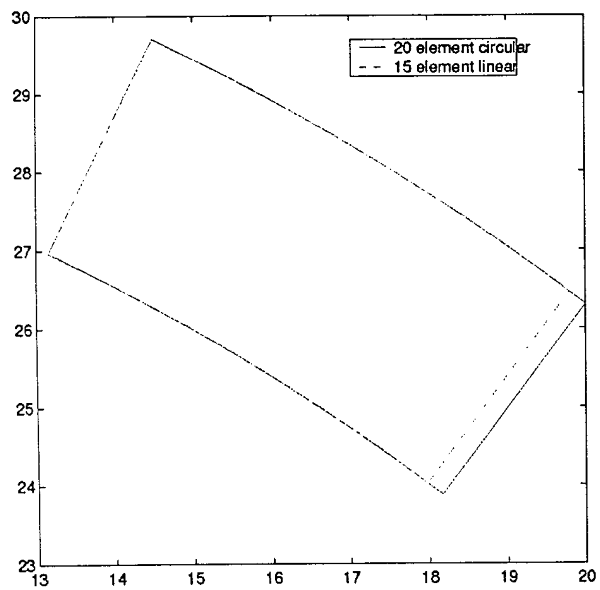

linear overlap percentage 1 PRI later: 99.2541
circular overlap percentage 1 PRI later: 99.254
percentage linear patch is of circular in same PRI: 95.9184
angular linear array patch length: 5.6541 km
angular circular array patch length: 5.8947 km
radial patch length: 40 m

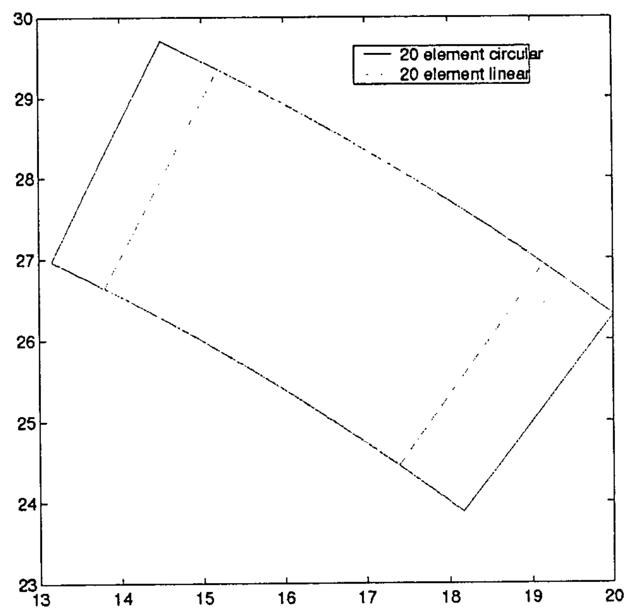

linear overlap percentage 1 PRI later: 99.2641
circular overlap percentage 1 PRI later: 99.254
percentage linear patch is of circular in same PRI: 71.4286
angular linear array patch length: 4.2105 km
angular circular array patch length: 5.8947 km
radial patch length: 40 m

NOTE: angular and radial distances not to scale

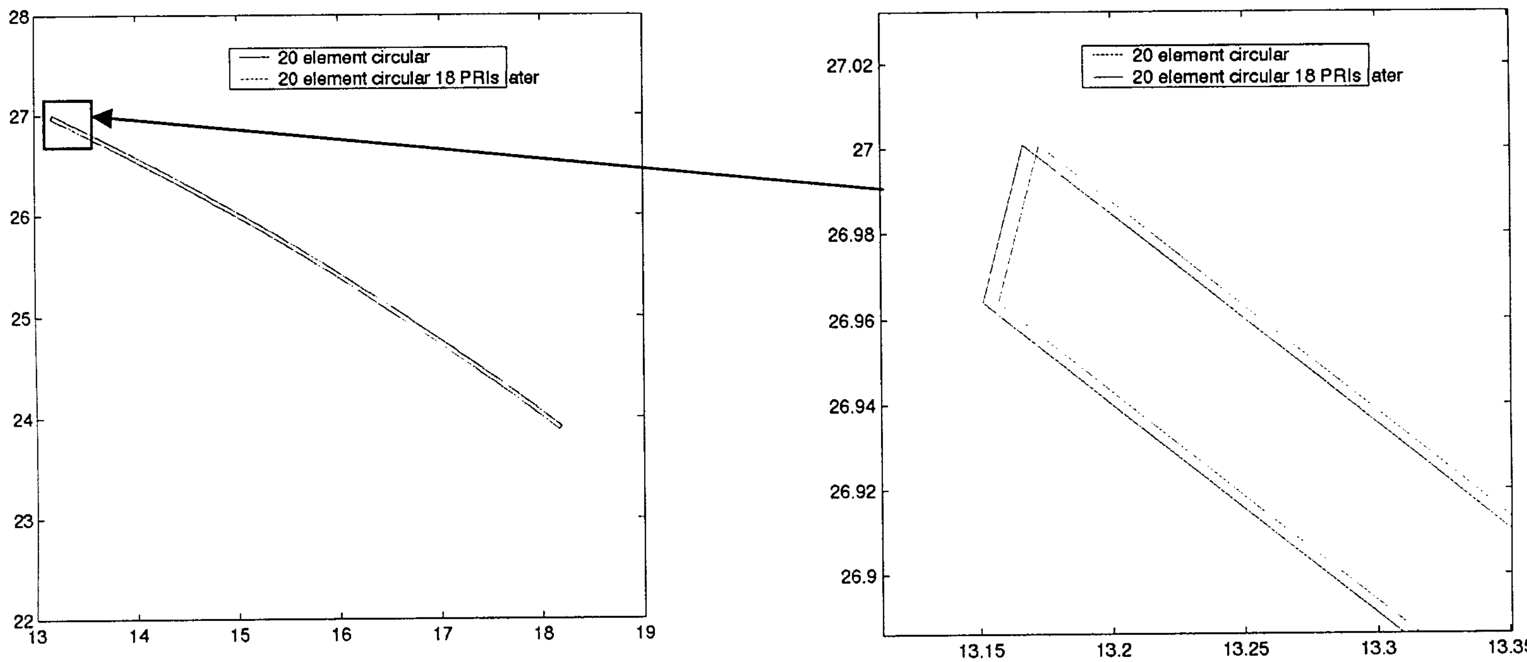

linear overlap percentage 18 PRIs later: 86.7447
circular overlap percentage 18 PRIs later: 86.5645

radial patch movement in 18 PRIs: 5.3279 m
angular patch movement in 18 PRIs: 2.7592 m

radial patch movement in 1 PRI: 0.2996 m
angular patch movement in 1 PRI: 0.14612 m